Dynamics of supercooled water in highly compacted clays studied by neutron scattering

2008 J. Phys.: Condens. Matter 20 415102

(http://iopscience.iop.org/0953-8984/20/41/415102)

IOP Publishing Journal of Physics: Condensed Matter

J. Phys.: Condens. Matter **20** (2008) 415102 (9pp) doi:10.1088/0953-8984/20/41/415102

Dynamics of supercooled water in highly compacted clays studied by neutron scattering

Fátima González Sánchez[1,6], Fanni Jurányi[2], Thomas Gimmi[1,3], Luc Van Loon[1], Tilo Seydel[4] and Tobias Unruh[5]

[1] Laboratory for Waste Management, Paul Scherrer Institute, CH-5232 Villigen PSI, Switzerland
[2] Laboratory for Neutron Scattering, Paul Scherrer Institute, CH-5232 Villigen PSI, Switzerland
[3] Institute of Geological Sciences, University of Bern, CH-3012 Bern, Switzerland
[4] Institut Laue-Langevin, 38042 Grenoble, France
[5] Forschungsneutronenquelle Heinz Maier-Leibnitz (FRM II), 85747 Garching, Germany

E-mail: fatima_oti@yahoo.com

Received 22 April 2008, in final form 3 July 2008
Published 5 September 2008
Online at stacks.iop.org/JPhysCM/20/415102

Abstract

The freezing behavior of water confined in compacted charged and uncharged clays (montmorillonite in Na- and Ca-forms, illite in Na- and Ca-forms, kaolinite and pyrophyllite) was investigated by neutron scattering. Firstly, the amount of frozen (immobile) water was measured as a function of temperature at the IN16 backscattering spectrometer, Institute Laue–Langevin (ILL). Water in uncharged, partly hydrophobic (kaolinite) and fully hydrophobic (pyrophyllite) clays exhibited a similar freezing and melting behavior to that of bulk water. In contrast, water in charged clays which are hydrophilic could be significantly supercooled. To observe the water dynamics in these clays, further experiments were performed using quasielastic neutron scattering. At temperatures of 250, 260 and 270 K the diffusive motion of water could still be observed, but with a strong reduction in the water mobility as compared with the values obtained above 273 K. The diffusion coefficients followed a non-Arrhenius temperature dependence well described by the Vogel–Fulcher–Tammann and the fractional power relations. The fits revealed that Na- and Ca-montmorillonite and Ca-illite have similar Vogel–Fulcher–Tammann temperatures (T_{VFT}, often referred to as the glass transition temperature) of ∼120 K and similar temperatures at which the water undergoes the 'strong–fragile' transition, $T_s \sim 210$ K. On the other hand, Na-illite had significantly larger values of $T_{VFT} \sim 180$ K and $T_s \sim 240$ K. Surprisingly, Ca-illite has a similar freezing behavior of water to that of montmorillonites, even though it has a rather different structure. We attribute this to the stronger hydration of Ca ions as compared with the Na ions occurring in the illite clays.

1. Introduction

The freezing and melting behavior of water and the dynamics of supercooled water in nanometer-sized pores have been a matter of attention in the last years (Christenson 2001, Liu *et al* 2006). Narrow pores, as occur for instance in clays, change the properties of pore water, such that the freezing partly occurs only at temperatures well below 273 K. The behavior of water in clays is of special interest, because clay rocks or compacted clays are widely considered as isolating barriers for radioactive waste disposal. Radionuclides can dissolve in water and escape by diffusion through the clay pores; therefore, it is essential to understand the specific water behavior.

[6] Author to whom any correspondence should be addressed. Present address: Mehrhaldenstrasse 8, CH-5415 Nussbaumen, Switzerland.

Clay minerals are nanoporous materials which offer a perfect environment (hydrophobic or hydrophilic) for the study of supercooled water. The presence of the clay surfaces and cations (chemical effect) and finite size constraints (physical effect) directly influence the water hydrogen bonding and thus the water dynamics and crystallization. Clay minerals belong to the phyllosilicates. They have a layered structure composed of planar sheets of Si^{4+} tetrahedra (T) and Al^{3+} or Mg^{2+} octahedra (O). Silicate clays are charged mainly due to isomorphic substitution, that is, the substitution of one element for another in the crystal sheets without change of the structure. This charge is compensated by positive counterions located in the interlayer spaces or near the external surfaces.

A large number of techniques have been employed to elucidate the structural and dynamical properties of supercooled water in confinement, e.g. x-ray and neutron diffraction (Yamaguchi *et al* 2006, Bellissent-Funel *et al* 1993), NMR (Mallamace *et al* 2006, Hwang *et al* 2007), and different neutron scattering techniques (Benham *et al* 1989, Venturini *et al* 2001). However, the microscopic mechanism of diffusion in supercooled water and the freezing/melting behavior of water near hydrophilic and hydrophobic surfaces (Bellissent-Funel 2005) are still poorly understood. Only a few studies (Bergman and Swenson 2000) exist at temperatures below 273 K about the water dynamics in swelling clays. These clays provide a two-dimensional geometry of interest for the study of water dynamics. Furthermore, there is no comparative study in the literature about the freezing/melting and dynamics of supercooled water in charged and uncharged clays.

Water confined in nanopores is unable to crystallize and remains fluid even below its homogeneous nucleation temperature $T_H = 235$ K (Chen *et al* 2006). Supercooled water becomes increasingly viscous towards its glass transition temperature, T_g—the temperature at which the water turns into an amorphous solid, generally believed to lie at about 135–140 K (Angell 2002). Typically, in a fluid the viscosity (η) and diffusion coefficients (D) in the supercooled region follow a super-Arrhenius temperature dependence such as the Vogel–Fulcher–Tammann (VFT) law (Vogel 1921, Fulcher 1925, Tammann and Hesse 1926):

$$D = D_0 e^{(-BT_{VFT}/(T-T_{VFT}))}, \quad (1)$$

where T is the temperature and B and D_0 are fitting constants. Liquids that present an Arrhenius behavior are termed 'strong', whereas liquids with a non-Arrhenius behavior are called 'fragile' (Angell 1988). According to another model, the diffusion coefficient of bulk water at temperatures below 273 K follows a fractional power law (FP) behavior (Bengtzelius *et al* 1984):

$$D = D_0 T^{1/2} \left(\frac{T}{T_s} - 1\right)^{\gamma}, \quad (2)$$

where γ is a fitting parameter and T_s is the low temperature limit, where D extrapolates to zero. It has been suggested that at temperatures below T_s bulk water ($T_s \sim 228$ K (Price *et al* 1999)) follows again an Arrhenius behavior. T_s is therefore the temperature at which the 'fragile–strong' transition occurs. Experimental studies showed that water confined in hydrophobic pores has a lower T_s value than when it is restrained in hydrophilic pores (Chu *et al* 2007). Investigations of water dynamics in clays (Bergman and Swenson 2000, Swenson *et al* 2001) revealed a non-Arrhenius behavior in the region below 273 K with a $T_{VFT} \approx 163$ K for a two-layer hydrated Na-vermiculite (swelling clay). Also, they suggested a fragile–strong transition at a singular temperature between $T_s = 215$–250 K.

Hysteresis of freezing and melting of water in confined porous media is a well known but not fully understood effect. It depends strongly on the pore size distribution, being significant in large pores and vanishing in small pores (Morishige and Kawano 1999). Moreover, hysteresis is related to the connectivity of the pores (Mu *et al* 1996), and the kinetics (temperature rate) of freezing and melting (Gleeson *et al* 1994). Freezing and melting hysteresis in cylindrical pores was explained by Grosse *et al* (1997) with the phenomenon of dynamic wetting of solids by liquids. An advancing wetting front always has a larger contact angle than a receding one, thus the freezing is lower than the melting temperature. As a result, interconnected pores showed a larger hysteresis than small and individual ones. The investigation of the hysteresis between the freezing and melting of water in clays with significantly different structure and chemistry could give more insight into the behavior of water at the supercooled conditions.

The especially large incoherent scattering cross section of hydrogen as compared to other elements makes neutron scattering a powerful technique to study the water dynamics in bulk or in restricted geometries such as nanoporous materials. We investigated the freezing/melting of charged and uncharged clays at the backscattering spectrometer IN16. The water diffusion below 273 K could be measured for the charged clays at the time of flight spectrometers FOCUS and TOFTOF, where supercooled water occurred. We then compared these data with values at temperatures > 273 K obtained in an earlier study (González Sánchez *et al* 2008a). The aim was to investigate the dynamics of water over a wide temperature range. The outcome of this study contributes to characterize (i.e. porosity) and get a better understanding of the fundamental transport processes (i.e. dominant influence of clay surfaces or cations) occurring in compacted clays.

2. Materials and method

Four different clays were investigated because of their different behavior in contact with water, namely montmorillonite from Milos (Decher 1997) and illite du Puy (Gabis 1958), both conditioned to the homoionic Na- and Ca-forms, kaolinite from Georgia (KGa-2 Van Olphen and Fripiat 1979), and pyrophyllite from North Carolina (Ward Natural Science 46E4630). The charged clays (montmorillonite and illite), with a TOT structure, have hydrophilic surfaces. In montmorillonite, which can swell upon addition of water, the water is located in between particles and in the interlayer space. In illite, which has no swelling capacity because the interlayer surfaces are tightly linked by potassium cations, water is located in between particles only. The uncharged clays were pyrophyllite (TOT structure) and kaolinite (TO structure). Pyrophyllite has hydrophobic surfaces (Bridgeman

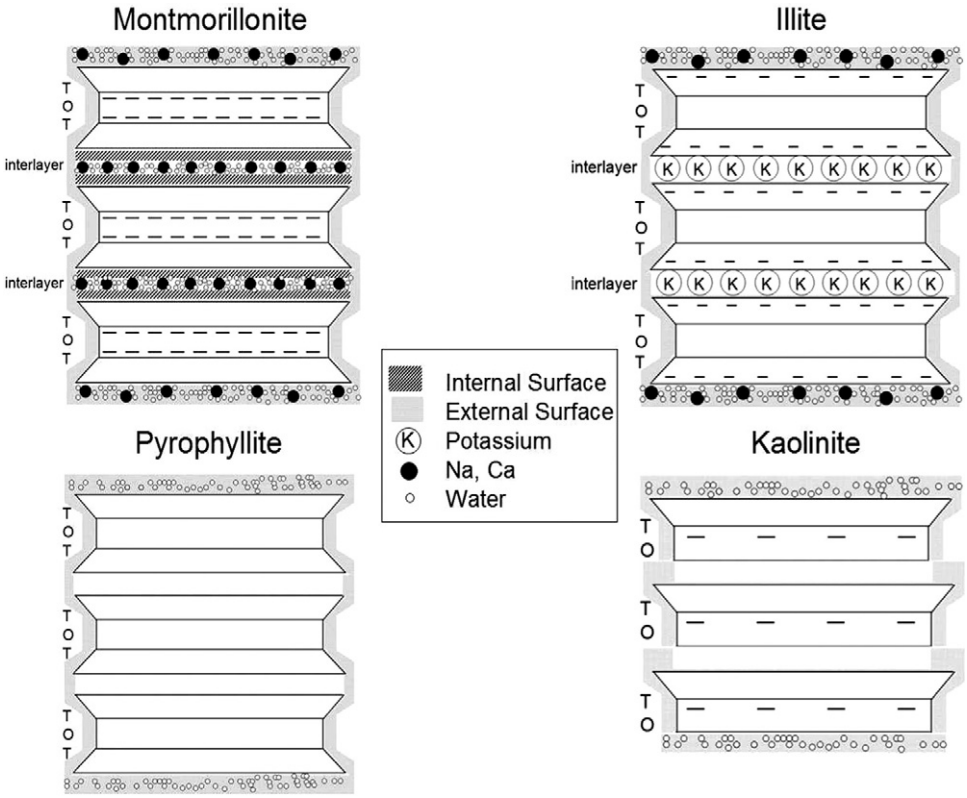

Figure 1. Schematic representation of the structures of the clays used. The small horizontal lines denote the negative charges present in the clay systems. Kaolinite has a very small permanent charge on the O layer, with a cation exchange capacity of 3.3 meq/100 g (Van Olphen and Fripiat 1979).

Table 1. Characterization of the hydrated pellets, after González Sánchez *et al* (2008a, 2008b). These clay parameters correspond to the water saturated samples.

Clays	Part. size (μm)	Porosity (%)	d-spacing (Å)	Water content (g/g)	Water layers	No of water molecules/cation
Na-mont.	0.50	32	14.79	0.16 ± 0.01	$\approx$2	8–9
Ca-mont.	1.10	30	15.35	0.15 ± 0.01	$\approx$2	16–18
Na-illite	0.32	28	9.92	0.14 ± 0.01	$\approx$9	30
Ca-illite	0.34	30	10.11	0.15 ± 0.01	$\approx$9	60
Kaolinite	1.30	26	7.16	0.13 ± 0.01	$\approx$20	—
Pyrophyllite[a]	1.30	30	9.2	0.15 ± 0.01	$\approx$60	—

[a] Pyrophyllite was only half saturated; a complete hydration was not possible due to its strong hydrophobic character.

and Skipper 1997); kaolinite is partly hydrophobic (T surface) and partly hydrophilic (O surface) (Tunega *et al* 2002). These clays have no interlayer space, so, the water is located only in between the particles (see figure 1).

An extensive characterization was performed by several experimental techniques in order to describe accurately the water–clay interaction at temperatures above 273 K (González Sánchez *et al* 2008a, 2008b). The most relevant parameters are shown in table 1. Compacted clays in a pellet form ($5 \times 1.5 \times 0.1$ cm^3 for montmorillonite and illite, and $5 \times 1.5 \times 0.2$ cm^3 for kaolinite and pyrophyllite), with a bulk dry density of $\rho_b = 1.85 \pm 0.05$ g cm^{-3}, were pressed from powders hydrated with the desired amount of water to get full saturation at this bulk density. After being measured, the samples were dried at 110 °C during 24 h in an evacuated furnace.

So-called fixed-window scans were performed at the backscattering spectrometer IN16 (ILL) (Frick and Gonzalez 2001). In this mode the Doppler drive was stopped, therefore the energy of the incident and scattered neutrons was the same. The intensity of these elastically scattered neutrons was measured as a function of temperature and it represents the amount of immobile or frozen water in the clay samples. The intensity of the dry samples was also measured at the same temperature range as the wet samples. Based on the IN16 experiments, several temperatures were selected to perform the study of the dynamics of water in charged clays (only hydrophilic surfaces) by quasielastic neutron scattering. The latter experiments were carried out at the chopper time-of-flight instrument TOFTOF (FRM II) (Unruh *et al* 2007) and at the hybrid time-of-flight spectrometer FOCUS (SINQ)

Table 2. Instrumental settings of the three set-ups used: incident wavelength, instrument resolution and Q range.

Instruments	λ_i (Å)	δE (μeV)	Q range (Å^{-1})
IN16	6.27	1	0.02–1.90
TOTOF	10	13	0.22–1.12
FOCUS	5.75	45	0.26–1.65

(Janssen *et al* 1997). The details of the instrumental settings are specified in table 2. The water saturated samples were kept in a watertight rectangular aluminum sample holder, placed at 45° slab angle (transmission). Vanadium was used to calibrate the detector efficiency and determine the energy resolution of the instruments. The dry samples and the empty sample holder were measured to account for the background. No quasielastic signal was observed for these dry clays, which shows that all diffusing water could be removed.

The obtained spectrum was dominated by the incoherent dynamic structure factor of the hydrogens in the water, $S_{\text{inc}}(Q, \omega)$. The translational motion of the supercooled water molecules could be described by a single Lorentzian with a half width at half maximum $\Gamma_t(Q)$. Additional data analysis including the rotational component led essentially to the same parameters for the translational diffusion. This is because in the temperature range studied (below 273 K), and in the energy range of interest for the translational diffusion, the rotational motion of the water molecules can be treated as a flat background. Therefore, assuming a three-dimensional, random, and spatially isotropic motion, the line width was fitted by the Singwi–Sjölander (Singwi and Sjolander 1960) and Hall–Ross (Hall and Ross 1981) models. The Singwi–Sjölander model assumes an exponential distribution of jump lengths and leads to

$$\Gamma_t(Q) = \frac{\hbar D_{SS} Q^2}{1 + D_{SS} Q^2 \tau_{t.SS}}, \tag{3}$$

whereas the Hall–Ross model is based on a Gaussian distribution of jump lengths, which results in

$$\Gamma_t(Q) = \frac{\hbar}{\tau_{t.HR}} \left[1 - \exp\left(-Q^2 D_{HR} \tau_{t.HR}\right)\right], \tag{4}$$

where $\hbar = 0.658$ eV ps is the reduced Planck constant, D the diffusion coefficient, and τ_t is the average residence time between two consecutive jumps.

The three-dimensional model of a translational diffusion described by a three-dimensional, random, and spatially isotropic motion is realistic for the water diffusion in illite clays. However, for montmorillonite it is valid only under certain circumstances. Most of the water contained in montmorillonite at this bulk density is located in the interlayer space (Pusch 2001), which provides a two-dimensional confinement. However, previous investigations of González Sánchez *et al* (2008a) in the range between 300 and 368 K revealed that for the current data the 3D model could be used to describe the local motion of the interlayer water because the instrument resolution is insufficient to capture the 2D diffusion. This applies even more for the lower temperatures used in this study.

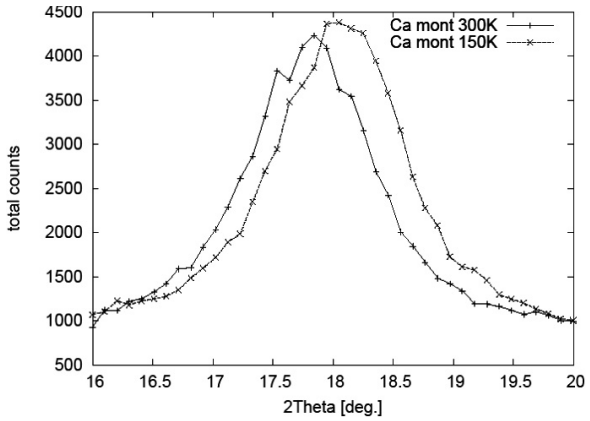

Figure 2. Differences of the two diffraction peaks (intensity versus 2θ) of Ca-montmorillonite at $T = 150$ and 300 K measured at the two-axis neutron diffractometer and reflectometer MORPHEUS. The calculated d-spacing at 150 K was 15.12 Å and that at 300 K was 15.33 Å.

We checked the variation of the interlayer space in montmorillonite produced by a temperature reduction through the two-axis neutron diffractometer and reflectometer MORPHEUS (http://kur.web.psi.ch/morpheus/) at the Paul Scherrer Institute, PSI. Figure 2 shows the differences of the two diffraction peaks of Ca-montmorillonite. The d-spacing at 150 K was 15.12 Å and that at 300 K was 15.33 Å. This variation (1.4%) is attributed to a change in the water density. We used 250 K as the lowest temperature for the study of the water dynamics; therefore a significantly smaller change is expected. We can then conclude that the diffusion coefficients calculated in Ca-montmorillonite at temperatures below 273 K were not influenced by a change in the interlayer space. Similar conclusions could be derived for Na-montmorillonite.

3. Results and discussion

3.1. Fixed-window scans

The intensity of the elastic scattering, which represents the amount of immobile or frozen water in the clay systems, is shown for uncharged clays in figure 3 and for charged clays in figure 4 as a function of temperature. The intensity difference between the wet and dry samples at each temperature should be correlated to the amount of liquid water in the samples. However, this difference was negative for $T > 273$ K (the intensity measured for the dry samples was higher than for the wet samples). The reason is that the neutron beam is attenuated while going through the sample. The quasielastic scattering originated from the diffusing water molecules acts as absorption. As a result, the intensity of the elastic scattering is reduced by the significant fraction of neutrons scattered at temperatures where water is still liquid. This effect is especially significant for the specific set-up of the instrument (backscattering), because the beam goes twice through the sample. Correction for this effect would be imprecise; therefore the data obtained for the dry clays were not used in the current analysis. Thus the curves shown in figures 3

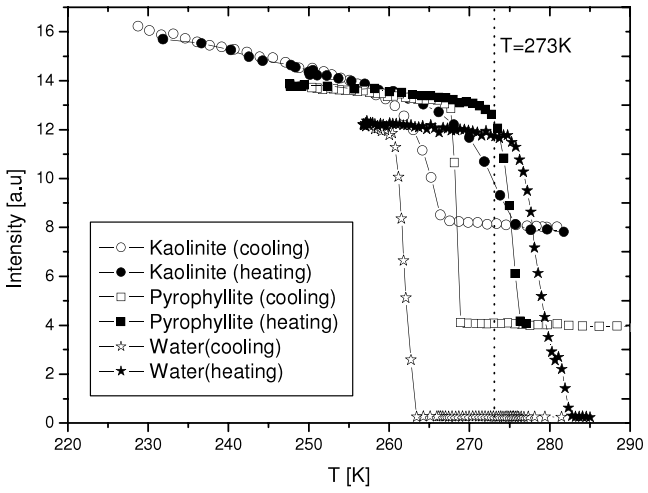

Figure 3. The elastic intensity for wet, uncharged clays and water measured as a function of temperature and summed up for all Q values. The heating and cooling rate for uncharged clays was $\sim$0.25 K min^{-1} and for water $\sim$0.5 K min^{-1}.

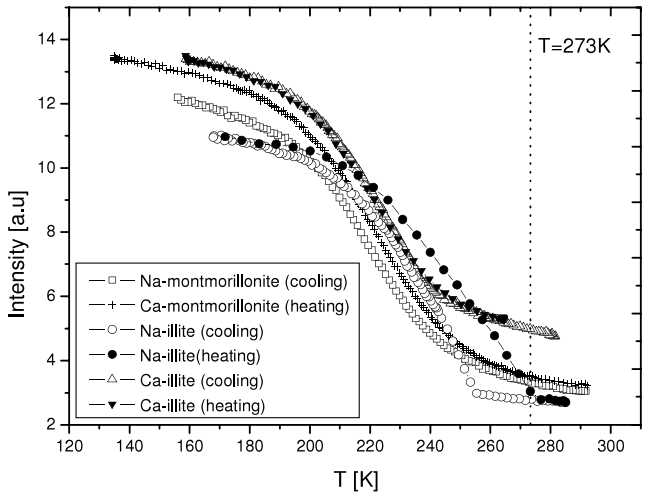

Figure 4. The elastic intensity for wet, charged clays measured as a function of temperature and summed up for all Q values. For the montmorillonites the cooling or heating branch is shown only, because these clays did not exhibit any hysteresis. The rates were $\sim$0.25 K min^{-1} and 1 K min^{-1} for cooling and heating, respectively.

and 4 correspond to the wet clays without any correction for the intensities of the dry samples.

As the samples were cooled down the elastic intensities showed an abrupt (uncharged clays) or gradual (charged clays) increase until the slope became relatively flat at about 260–265 K (uncharged clays) or 180–190 K (charged clays). This increase in the elastic intensities indicates a decrease in the quasielastic signal of liquid water until at sufficiently low temperatures the quasielastic line falls entirely into the energy window given by the instrument resolution. Below this temperature the variation in the elastic signal is only due to the Debye–Waller factor, which represents the number of inelastically scattered neutrons caused by thermal vibrations.

The stronger hydrophobic character of pyrophyllite as compared to kaolinite (also partly hydrophilic Tunega *et al* 2002) was observed in the freezing curves. The water in pyrophyllite freezes homogeneously, as predicted for other hydrophobic surfaces (Koga and Tanaka 2005), whereas in kaolinite this process is smoother.

Geometrical restrictions and chemical interactions of water in clays prevent water crystallization at temperature $<$ 273 K. In the uncharged clays, the chemical effects are negligible. There, we conclude from the freezing curves (figure 3) that the pores should be larger in pyrophyllite than in kaolinite. This is in agreement with the estimated average number of water layers between the clay surfaces shown in table 1.

The freezing behavior of the charged clays is significantly affected by both the chemical and the geometrical effects. It is well established that aqueous solutions freeze at lower temperature than bulk water depending on the concentration of the solute. According to figure 4, Na- and Ca-montmorillonite had a very similar freezing behavior, despite the large differences of the hydration properties of Na and Ca cations (Ohtaki and Radnai 1993). Therefore the geometrical constraints of the interlayer spaces seemed to be dominant here. The two forms of illite, however, presented significant differences in the freezing curves. Na-illite had a noticeable hysteresis and a certain similarity to the behavior of the uncharged clays, whereas Ca-illite was very similar to the montmorillonites. This similarity was rather unexpected and is interpreted as being due to the different hydration properties of the saturating cations in the illite samples. Both illites have the same particle size, porosity, and number of water layers between particles (see table 1) and produce stacks of the same size (Poinssot *et al* 1999). In illite the cations are fully hydrated and thus have a larger influence on the pore water than in montmorillonite, where the confinement (interlayer) does not allow a full hydration of cations.

Bulk water showed hysteresis, which could be caused by the kinetics while cooling or heating (0.5 K min^{-1}). The same effect was also observed in the uncharged clays (0.25 K min^{-1} cooling and heating), where the confined water has a more bulk-like behavior. In the case of charged clays, no hysteresis was found except for Na-illite. The difference in hysteresis in both illites proved that with surfaces and cations interacting with the fluid, a purely geometrical description (Morishige and Kawano 1999, Mu *et al* 1996) of the hysteresis cannot be valid.

The differences in the freezing behavior are in agreement with the results and conclusions of previous QENS studies for the same clays at temperatures above 273 K. González Sánchez *et al* (2008a) found that the two forms of montmorillonite had similar dynamical behavior, whereas Ca-illite showed a much more reduced water motion than the Na-illite. However, Ca-illite was not so similar to montmorillonite as in this study.

3.2. QENS dynamics

Quasielastic neutron scattering experiments were performed for the charged clays at 250, 260 and 270 K. A plot showing the quality of the fits is presented in figure 5. The diffusion coefficients and residence times of the charged clays are shown in table 3. For comparison purposes table 4 shows the same

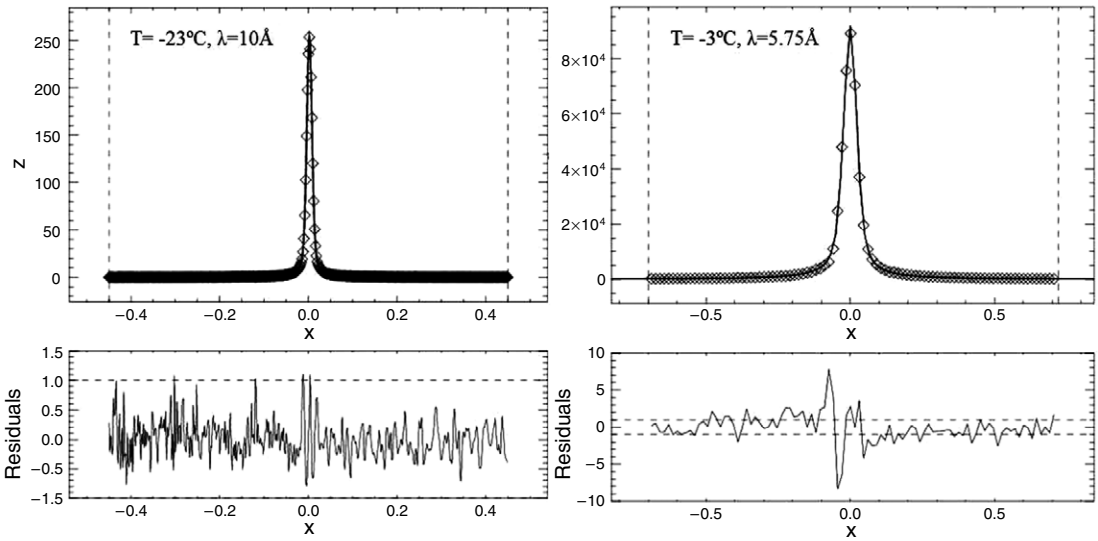

Figure 5. Quality of the fits of the intensity (arbitrary units) versus exchanged energy (meV) for Ca-illite at $Q = 0.7$ Å^{-1} for $T = 250$ K (left-hand side) and $T = 270$ K (right-hand side).

Table 3. Translational diffusion coefficients D (m^2 s^{-1}) and residence times τ_t (ps) for Na-montmorillonite (Na-m), Ca-montmorillonite (Ca-m), Na-illite (Na-i) and Ca-illite (Ca-i) calculated at different temperatures by the Singwi–Sjölander (SS) and Hall–Ross (HR) jump diffusion models. Ca-montmorillonite at $T = 250$ K was measured at FOCUS ($\lambda = 5.75$ Å), where the resolution was at the limit of the detection of dynamical effects. Therefore, these particular results are less reliable and have a larger error.

Clay	T (K)	λ_i (Å)	D_{SS} ($\times 10^{-10}$ m^2 s^{-1})	$\tau_{t.SS}$ (ps)	D_{HR} ($\times 10^{-10}$ m^2 s^{-1})	$\tau_{t.HR}$ (ps)
Na-m	250	10	3.55 ± 0.14	32.61 ± 1.23	3.20 ± 0.13	44.00 ± 1.02
Na-m	260	5.75	5.14 ± 0.23	22.44 ± 1.44	4.30 ± 0.22	29.11 ± 0.88
Na-m	270	5.75	6.40 ± 0.24	17.24 ± 0.87	5.30 ± 0.26	22.38 ± 1.01
Ca-m	250	5.75	3.70 ± 1.0	32.30 ± 9.0	3.20 ± 1.0	41.18 ± 16.0
Ca-m	260	5.75	5.07 ± 0.20	20.72 ± 1.04	4.25 ± 0.31	27.18 ± 0.94
Ca-m	270	5.75	6.51 ± 0.27	17.06 ± 0.46	5.42 ± 0.28	22.21 ± 0.77
Na-i	250	10	3.11 ± 0.15	23.22 ± 1.34	3.00 ± 0.21	37.43 ± 1.36
Na-i	260	5.75	6.20 ± 0.27	12.27 ± 0.83	5.50 ± 0.19	16.84 ± 1.42
Na-i	270	5.75	8.24 ± 0.23	7.98 ± 0.76	7.73 ± 0.29	11.42 ± 0.49
Ca-i	250	10	3.32 ± 0.15	27.28 ± 1.35	3.16 ± 0.17	42.53 ± 1.84
Ca-i	260	5.75	5.48 ± 0.25	16.24 ± 0.87	4.65 ± 0.23	21.57 ± 1.64
Ca-i	270	5.75	7.80 ± 0.27	11.15 ± 0.61	6.70 ± 0.26	14.99 ± 0.65

parameters at similar temperatures for bulk water as found in the literature.

The two jump diffusion models (Singwi–Sjölander and Hall–Ross) described the data equally well (see figure 6). The diffusion coefficients are always 10–20% larger for the Singwi–Sjölander than for the Hall–Ross model. The opposite behavior was found for the time between jumps τ_t, that is, 10–20% larger values for the Hall–Ross than for the Singwi–Sjölander model.

The water dynamics in Na- and Ca-montmorillonite at temperatures below 273 K was very similar, as was also the case above 273 K (González Sánchez *et al* 2008a). At the studied degree of compaction more than 95% of the water is contained in the interlayers (Pusch 2001). Here, the effect of the cations is hidden because of the spatial restrictions (interlayers), which impede the full hydration of the cations.

The influence of the cations on the water dynamics was well observed in the case of illite for $T = 270$ and 260 K similarly as at temperatures above 273 K (González Sánchez *et al* 2008a). Ca-illite had a lower D and a larger τ_t than the Na-form. At $T = 250$ K this difference disappeared and both illite forms presented similar dynamics. The smaller amount of unfrozen, mobile water in the Na-illite seemed to

Table 4. Translational diffusion coefficients D (m^2 s^{-1}), residence times τ_t (ps), activation energy E_a (kJ mol^{-1}) at temperatures above and below 273 K, glass T_g (K), and 'fragile–strong' transition temperatures T_s (K) for bulk water.

T (K)	D [a] ($\times 10^{-10}$ m^2 s^{-1})	τ_t [a] (ps)
253	4.19	22.7
263	7.01	6.47
268	8.48	4.66
T_g [b] (K) = 135–140	T_s [c] (K) = 228	E_a [d,e] (>273 K) = 17 ± 1 kJ mol^{-1}
		E_a [c] (250 K) = 30 kJ mol^{-1}

[a] After Teixeira *et al* (1985).
[b] After Angell (2002).
[c] After Price *et al* (1999).
[d] After Wang (1951).
[e] After Low (1962).

Table 5. Glass T_g (K) and 'fragile–strong' transition temperatures T_s (K), and activation energies E_a (kJ mol^{-1}) for the two data sets obtained by Singwi–Sjölander (SS) and Hall–Ross (HR) models. The clays were fitted at the temperature range of 250–368 K. The E_a data for the values of 368–300 K were taken from the QENS study of González Sánchez *et al* (2008a). The abbreviations correspond to Na-montmorillonite (Na-m), Ca-montmorillonite (Ca-m), Na-illite (Na-i), and Ca-illite (Ca-i).

Clay	$T_{g(SS)}$ (K)	$T_{g(HR)}$ (K)	$T_{s,SS}$ (K)	$T_{s,HR}$ (K)	$E_{a(SS)}$ T (300–368 K)	$E_{a(HR)}$ T (300–368 K)	$E_{a(SS)}$ T (250 K)	$E_{a(HR)}$ T (250 K)
Na-m	108 ± 22	76 ± 24	205 ± 15	195 ± 15	11.8 ± 1.0	11.8 ± 1.0	16.1 ± 1.0	14.6 ± 1.0
Ca-m	107 ± 11	75 ± 14	201 ± 7	188 ± 9	11.6 ± 1.2	11.8 ± 1.0	16.0 ± 0.5	14.4 ± 0.5
Na-i	188 ± 6	183 ± 5	238 ± 4	240 ± 4	12.5 ± 0.3	12.8 ± 0.3	35.7 ± 2.0	33.9 ± 1.0
Ca-i	134 ± 16	100 ± 19	200 ± 15	176 ± 28	14.8 ± 0.3	15.6 ± 0.3	23.4 ± 0.5	20.5 ± 0.5

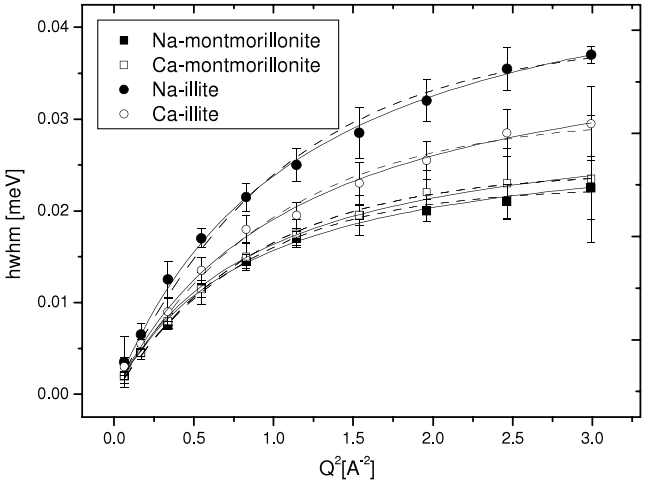

Figure 6. The measured Γ_t (meV) versus Q^2 (Å^{-2}) symbols and the fits of the two models, Singwi–Sjölander (solid line) and Hall–Ross (dashed line), at $T = 260$ K and $\lambda = 5.75$ Å for the charged clays.

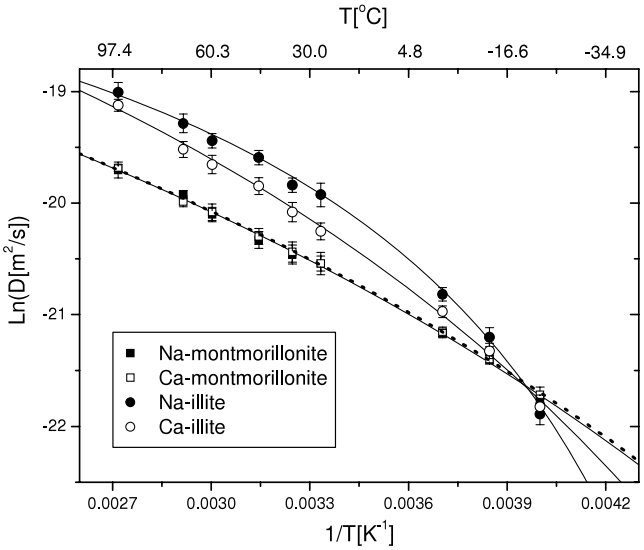

Figure 7. The temperature dependence of the diffusion coefficients for the charged clays fitted by the VFT law for the data set obtained by the Singwi–Sjölander model. The dashed line corresponds to the fit of Ca-montmorillonite. The data for the values above 273 K were taken from the QENS study of González Sánchez *et al* (2008a).

reduce the water mobility to diffusion coefficients closer to the Ca-illite.

The water motion in the supercooled region for all the clays studied showed a remarkable reduction in the diffusion coefficients as compared with bulk water and a large increase in the residence times (table 4). The jump diffusion lengths ($l = \sqrt{6D\tau}$) were very similar for all the temperatures, including the previous studied temperatures above 273 K (González Sánchez *et al* 2008a), for the two types of montmorillonite (2.7 Å) and Ca-illite (2.4 Å). Na-illite (2.2 Å) had ∼20% larger l in the supercooled region than above 273 K. The reason for this difference remains unclear.

3.3. Activation energies and glass transition temperatures

The temperature dependence of the diffusion coefficients obtained in a previous study for temperatures above 273 K (González Sánchez *et al* 2008a) showed an Arrhenius behavior; however, the data of the supercooled region followed a super-Arrhenius behavior. These data were extended to 250 K; further down to this temperature a mixture of different fractions of water and ice can be found within the clay pores (see figure 4). Therefore the diffusion coefficients, which describe an average of this inhomogeneous water–ice system, could not be compared. The extended data set, down to 250 K, could be equally well fitted over the whole temperature range (250–368 K) by two different models: the Vogel–Fulcher–Tammann (VFT) (equation (1)) and the fractional power (FP) (equation (2)). However, we expect a divergence of the two models near to the critical temperatures (T_{VFT} and T_s), as happens in bulk water (Price *et al* 1999). The obtained parameters are presented in table 5, and figure 7 shows the VFT fits.

Through the fit of the VFT model we obtained T_{VFT} (also referred to by some authors as the glass transition temperature). with values very similar for Na- and Ca-montmorillonite and Ca-illite ($T_{VFT} \approx 120$ K). However, Na-illite showed a larger value, $T_{VFT} \approx 180$ K, which is in agreement with the freezing curves, where Na-illite seemed to freeze at higher temperatures than Na- and Ca-montmorillonite and Ca-illite.

Both montmorillonites and Ca-illite had a $T_s \approx 210$ K obtained through the FP fit. Na-illite had a value, $T_s \approx 240$ K, slightly higher than that of bulk water (see table 4). The results are comparable with those obtained for a two-layer hydrated Na-vermiculite, where $T_{VFT} = 163$ K and $T_s \approx 215$–250 K (Swenson *et al* 2001).

By taking the derivative of equation (1), we could obtain the activation energy (table 4) for the diffusive processes at the

studied supercooled temperatures by the following expression:

$$E_a = \frac{BT_{\mathrm{VFT}}R}{(1-(T_{\mathrm{VFT}}/T))^2}, \quad (5)$$

with $R = 8.314$ J K^{-1} mol^{-1} the molar gas constant, and B a fitting parameter, as obtained for the VFT fit. The activation energy values followed the increasing order Na-montmorillonite ≈ Ca-montmorillonite < Ca-illite < water < Na-illite (tables 4 and 5). The values obtained at temperatures in the supercooled regime were significantly larger than the activation energies obtained at temperatures above 273 K (González Sánchez *et al* 2008a). The clays Na- and Ca-montmorillonite and Ca-illite had lower activation energies than that of bulk water above and below 273 K; however, Na-illite had lower activation energy above 273 K and slightly higher below this temperature.

As the temperature range went no further down than 250 K to the region where typically T_{VFT} and T_{s} occur, the values obtained for these two parameters as well as for the activation energies (below 273 K) remain uncertain. However, these data are consistent with the observations of the freezing curves (figure 4).

4. Conclusions and discussion

The fixed-window scans showed that water in uncharged clays freezes significantly differently from the water in charged clays. Charged clays showed a smooth and gradual freezing of water, whereas uncharged clays had a more bulk-water-like freezing behavior. Hysteresis effects were present in kaolinite, pyrophyllite and Na-illite but not in Na- or Ca-montmorillonite or Ca-illite. The data showed that geometrical and chemical effects have to be taken into account, and their significance depends on the particular clay structure. The dynamics of water in charged clays in the supercooled regime showed a strong reduction of D and a large increase of τ_{t} as compared with bulk water. For Na- and Ca-montmorillonite and Ca-illite the jump length remained the same as the values found for temperatures above 273 K (González Sánchez *et al* 2008a). The clays studied in the supercooled regime could be equally well described by the super-Arrhenius Vogel–Fulcher–Tammann (VFT) and fractional power (FP) relations at the studied temperature range (250–368 K). Within the charged clays Na- and Ca-montmorillonite and Ca-illite showed strong similarities in the freezing behavior and dynamics of water. This group showed similar values for T_{VFT} and T_{s}, in contrast to Na-illite, which had a behavior closer to that of bulk water. The similarities of these three clays (Na- and Ca-montmorillonite and Ca-illite) contrasted with the large structural differences of montmorillonite as compared to illite. Montmorillonite has a significantly number amount of cations and notably smaller average pore size than the Ca-illite. It seems that for the montmorillonites the reactive surfaces dominate the freezing behavior, whereas for the Ca-illite at the given density the chemical effects of the dissolved cation are also responsible for the observed freezing depression.

Acknowledgments

The authors would like to thank B Baeyens and U Berner for many helpful discussions. Additional thanks go to J Stahn for the measurements at MORPHEUS. This work is based on experiments performed at the Swiss spallation neutron source SINQ, Paul Scherrer Institute, Villigen, Switzerland; FRM II, Garching, Germany; and ILL, Grenoble, France.

References

Angell C A 1988 Perspective on the glass-transition *J. Phys. Chem. Solids* **49** 863–71
Angell C A 2002 Liquid fragility and the glass transition in water and aqueous solutions *Chem. Rev.* **102** 2627–49
Bellissent-Funel M C, Lal J and Bosio L 1993 Structural study of water confined in porous-glass by neutron-scattering *J. Chem. Phys.* **98** 4246–52
Bellissent-Funel M C 2005 Hydrophilic–hydrophobic interplay: from model systems to living systems *C. R. Geosci.* **337** 173–9
Bengtzelius U, Gotze W and Sjolander A 1984 Dynamics of supercooled liquids and the glass-transition *J. Phys. C: Solid State Phys.* **17** 5915–34
Benham M J, Cook J C, Li J C, Ross D K, Hall P L and Sarkissian B 1989 Small-angle neutron-scattering study of adsorbed water in porous vycor glass—supercooling phase-transition and interfacial structure *Phys. Rev.* B **39** 633–6
Bergman R and Swenson J 2000 Dynamics of supercooled water in confined geometry *Nature* **403** 283–6
Bridgeman C H and Skipper N T 1997 A Monte Carlo study of water at an uncharged clay surface *J. Phys.: Condens. Matter* **9** 4081–7
Chen S H, Mallamace F, Mou C Y, Broccio M, Corsaro C, Faraone A and Liu L 2006 The violation of the Stokes–Einstein relation in supercooled water *Proc. Natl Acad. Sci. USA* **103** 12974–8
Christenson H K 2001 Confinement effects on freezing and melting *J. Phys.: Condens. Matter* **13** R95–133
Chu X-Q, Kolesnikov A I, Moravsky A P, Garcia-Sakai V and Chen S-H 2007 Observation of a dynamic crossover in water confined in double-wall carbon nanotubes *Phys. Rev.* E **76** 021505
Decher A (ed) 1997 Bentonite der Insel Milos, Griechenland *Doctoral Thesis* TH Aachen (Germany) ISBN: 3-86073-602-7
Frick B and Gonzalez M 2001 Five years operation of the second generation backscattering spectrometer IN16-a retrospective, recent developments and plans *Physica* B **301** 8–19
Fulcher G S 1925 Analysis of recent measurements of the viscosity of glasses *J. Am. Ceram. Soc.* **8** 339–55
Gabis V 1958 Etude préliminaire des argiles oligocènes du Puy-en-Velay (Haute-Loire) *Bull. Soc. Franç. Minéral. Cristallog.* **81** 183–5
Gleeson J T, Erramilli S and Gruner S M 1994 Freezing and melting water in lamellar structures *Biophys. J.* **67** 706–12
González Sánchez F, Jurányi F, Gimmi T, Van Loon L, Unruh T and Diamond L W 2008a Translational diffusion of water and its dependence on temperature in charged and uncharged clays: a neutron scattering study *J. Chem. Phys.* submitted
González Sánchez F, Van Loon L, Gimmi T, Jakob A and Glaus M 2008b Self diffusion of water and its dependence on temperature and ionic strength in highly compacted montmorillonite, illite and kaolinite *Appl. Geochem.* at press
Grosse K, Ratke L and Feuerbacher B 1997 Solidification and melting of succinonitrile within the porous network of an aerogel *Phys. Rev.* B **55** 2894–902
Hall P L and Ross D K 1981 Incoherent neutron-scattering functions for random jump diffusion in bounded and infinite media *Mol. Phys.* **42** 673–82

Hwang D W, Chu C C, Sinha A K and Hwang L P 2007 Dynamics of supercooled water in various mesopore sizes *J. Chem. Phys.* **126** 044702

Janssen S, Mesot J, Holitzner L, Furrer A and Hempelmann R 1997 FOCUS: a hybrid TOF-spectrometer at SINQ *Physica* B **234** 1174–6

Koga K and Tanaka H 2005 Phase diagram of water between hydrophobic surfaces *J. Chem. Phys.* **122** 104711

Liu L, Chen S H, Faraone A, Yen C W, Mou C Y, Kolesnikov A I, Mamontov E and Leao J 2006 Quasielastic and inelastic neutron scattering investigation of fragile-to-strong crossover in deeply supercooled water confined in nanoporous silica matrices *J. Phys.: Condens. Matter* **18** S2261–84

Low P F 1962 Influence of absorbed water on exchangeable ion movement *Clays Clay Miner.* **9** 219–28

Mallamace F, Broccio M, Corsaro C, Faraone A, Liu L, Mou C Y and Chen S H 2006 Dynamical properties of confined supercooled water: an NMR study *J. Phys.: Condens. Matter* **18** S2285–97

Morishige K and Kawano K 1999 Freezing and melting of water in a single cylindrical pore: the pore-size dependence of freezing and melting behavior *J. Chem. Phys.* **110** 4867–72

Mu R, Xue Y, Henderson D O and Frazier D O 1996 Thermal and vibrational investigation of crystal nucleation and growth from a physically confined and supercooled liquid *Phys. Rev.* B **53** 6041–7

Ohtaki H and Radnai T 1993 Structure and dynamics of hydrated ions *Chem. Rev.* **93** 1157–204

Poinssot C, Baeyens B and Bradbury M H 1999 Experimental studies of Cs, Sr, Ni, and Eu sorption on Na-illite and the modelling of Cs sorption *PSI Technical Report 99-06* (Villigen, Switzerland: Paul Scherrer Institute, PSI) ISSN 1019-0643

Price W S, Ide H and Arata Y 1999 Self-diffusion of supercooled water to 238 K using PGSE NMR diffusion measurements *J. Phys. Chem.* A **103** 448–50

Pusch R 2001 The microestructure of MX-80 clay with respect to its bulk physical properties under different enviromental conditions SKB *Technical Report TR-01-08 (Swedish Nuclear Fuel and Waste Management Co. (SKB))* ISSN 1404-0344

Singwi K S and Sjolander A 1960 Diffusive motions in water and cold neutron scattering *Phys. Rev.* **119** 863–71

Swenson J, Bergman R and Longeville S 2001 A neutron spin-echo study of confined water *J. Chem. Phys.* **115** 11299–305

Tammann G and Hesse W 1926 Die abhangigkeit der viskositat von der temperatur bei unterkuhlten flussigkeiten *Z. Anorg. Allg. Chem.* **156** 245–57

Teixeira J, Bellissent-Funel M C, Chen S H and Dianoux A J 1985 Experimental determination of the nature of diffusive motions of water molecules at low temperatures *Phys. Rev.* A **31** 1913–7

Tunega D, Haberhauer G, Gerzabek M H and Lischka H 2002 Theoretical study of adsorption sites on the (001) surfaces of 1: 1 clay minerals *Langmuir* **18** 139–47

Unruh T, Neuhaus J and Petry W 2007 The high-resolution time-of-flight spectrometer TOFTOF *Nucl. Instrum. Methods* **580** 1414–22

Van Olphen H and Fripiat J J (ed) 1979 *Data Hand Book for Clay Minerals* (Oxford: Pergamon) ISBN-0-08-022850-0-X

Venturini F, Gallo P, Ricci M A, Bizzarri A R and Cannistraro S 2001 Low frequency scattering excess in supercooled confined water *J. Chem. Phys.* **114** 10010–4

Vogel H 1921 Temperaturabhängigkeitsgesetz der viskosität von flüssigkeite *Phys. Z.* **22** 645–6

Wang J H 1951 Self-diffusion and structure of liquid water 1 measurement of self-diffusion of liquid water with deuterium as tracer *J. Am. Chem. Soc.* **73** 510–13

Yamaguchi T, Hashi H and Kittaka S 2006 X-ray diffraction study of water confined in activated carbon pores over a temperature range of 228–298 K *J. Mol. Liquids* **129** 57–62